 Nucleic Acids Research, 1999, Vol. 27, No. 21 **4235–4240**

RPA subunit arrangement near the 3′-end of the primer is modulated by the length of the template strand and cooperative protein interactions

Olga I. Lavrik*, Dmitry M. Kolpashchikov, Klaus Weisshart[1], Heinz-Peter Nasheuer[1], Svetlana N. Khodyreva and Alain Favre[2]

Novosibirsk Institute of Bioorganic Chemistry Siberian Division of Russian Academy of Sciences, Prospect Lavrentiev 8, 630090 Novosibirsk, Russia, [1]Institut für Moleculare Biotechnologie, D-07708 Jena, Germany and [2]Institut Jacques Monod (CNRS, Universitè Paris 6, Universitè Paris 7), 75351 Paris Cedex 05, France

Received June 25, 1999; Revised August 19, 1999; Accepted September 16, 1999

ABSTRACT

To analyze the interaction of human replication protein A (RPA) and its subunits with the DNA template–primer junction in the DNA replication fork, we designed several template–primer systems differing in the size of the single-stranded template tail (4, 9, 13, 14, 19 and 31 nt). Base substituted photoreactive dNTP analogs—5-[*N*-(2-nitro-5-azidobenzoyl)-*trans*-3-aminopropenyl-1]-2′-deoxyuridine-5′-triphosphate (NAB-4-dUTP) and 5-[*N*-[*N*-(2-nitro-5-azidobenzoyl)glycyl]-*trans*-3-aminopropenyl-1]-2′-deoxyuridine-5′-triphosphate (NAB-7-dUTP)—were used as substrates for elongation of radiolabeled primer–template by DNA polymerases in the presence or absence of RPA. Subsequent UV crosslinking showed that the pattern of p32 and p70 RPA subunit labeling, and consequently their interaction with the template–primer junction, is strongly dependent on the template extension length at a particular RPA concentration, as well as on the ratio of RPA to template concentration. Our results suggest a model of changes in the RPA configuration modulating by the length of the template extension in the course of nascent DNA synthesis.

INTRODUCTION

The eukaryotic single-stranded DNA (ssDNA) binding protein, replication protein A (RPA), is a stable heterotrimer consisting of subunits with molecular masses of 70, 32 and 14 kDa, correspondingly called p70, p32 and p14. This protein has multiple functions in various processes of DNA metabolism (reviewed in 1). RPA is required during the initiation and elongation stages of DNA replication and is involved in both DNA repair and recombination.

The interaction of RPA with ssDNA has been extensively studied. The major ssDNA binding activity of RPA belongs to the p70 subunit (1). It has been shown that a total of three independent DNA binding sites exist in this subunit, which have been designated domains A, B and C, respectively (2). Crystallographic studies of a subfragment of p70 comprising domains A and B confirmed that both are indeed involved in ssDNA binding (3). The role of DNA binding domains located on the p70 RPA subunit in both double-stranded DNA (dsDNA) binding and helix destabilization was examined recently (4,5). The fourth DNA binding domain, domain D, of RPA resides in the p32 subunit (2,6). The p32 subunit can be crosslinked to ssDNA, although only as part of the RPA complex and only at low efficiency (7). In the complex with p14 alone, the activity of the ssDNA binding domain was only revealed if the subunit was truncated N- and C-terminally (6). Interaction of the p32 subunit of RPA with nascent DNA in replicating SV40 chromosomes indicates that the p32 subunit contacts early intermediates produced by DNA polymerase α–primase but not more advanced products (8).

Different modes of RPA binding to ssDNA have been reported whereby RPA shows different occlusion sites (9–12). For human RPA two different kinds of DNA complexes have been found, those in which RPA occupies stretches of 8–10 and 30 nt, forming the so-called 8 nt and 30 nt complexes (10,11). These complexes exhibit different affinity for DNA (10). In addition, scanning electron microscopy has revealed structural differences between these RPA–DNA complexes, which depend on both protein–protein interactions and the available length of ssDNA for RPA binding. The 30 nt complex appeared to be more elongated and exists as contracted and extended structures, respectively. Based on the stability of the complexes it was hypothesized that the globular and the contracted elongated forms represent binding transition states to the extended elongated form in which RPA is bound to DNA more stably (10,11).

Although the study of the interactions of RPA with various ssDNA templates is well advanced it cannot tell us much about the interactions of RPA with DNA during the process of DNA replication. A DNA duplex with an extended template strand is more informative since such a primer–template configuration represents an appropriate model of the DNA structure operating at the replication fork. One of the most promising techniques for analyzing RPA subunit arrangement around such a DNA template is the method of photoaffinity labeling. Photoreactive primers have been synthesized *in situ* by DNA polymerases by using base substituted dNTPs carrying photoreactive arylazido

*To whom correspondence should be addressed. Tel: +7 3832 344296; Fax: +7 3832 333677; Email: lavrik@niboch.nsc.ru

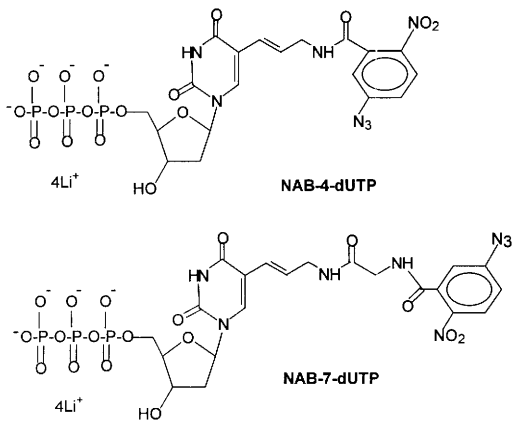

Figure 1. Structural formulae of photoreactive dUTP analogs. The photoreactive arylazido group of NAB-4-dUTP and NAB-7-dUTP is attached to the nucleotide by a spacer of 10 and 12 Å, respectively.

groups that permit the introducion of a photoreactive group at the 3′-end of the primer (13,14). This technique proved to be a powerful tool to identify various complexes of RPA with DNA and evaluate RPA subunit arrangement near the template–primer junction even when these structures are not stable enough to be studied by other techniques (13,14). In addition, it has been demonstrated by us that the pattern of subunit labeling is changed when the template extension is shortened (13).

In the present work we varied the template extension length systematically to find the length of single-stranded template tail that induces the transition in RPA conformation. This resulted in varying efficiencies of p32 and p70 interaction with the template–primer junction. To analyze cooperative RPA binding to DNA, we changed the RPA:DNA duplex concentration ratio. We demonstrated with these experiments that the RPA configuration was strongly dependent on both the template extension length, and the RPA:DNA ratio. The data revealed a template-dependent transition of RPA conformation when the p70 subunit bound to the single-stranded tail of the template became more accessible to the 3′-end of the primer than p32. Such a transition might take place as the template strand becomes shorter in the course of nascent DNA synthesis.

MATERIALS AND METHODS

Proteins and nucleotides

Recombinant polymerase β (pol β) and the Klenow fragment of *Escherichia coli* DNA polymerase I (KF) were purified according to Beard and Wilson (15) and Joyce and Grindley (16), respectively. RPA was expressed in *E.coli* and purified as described (17,18). Rainbow colored protein molecular mass markers were from Amersham. [γ-^{32}P]ATP was from ICN. Synthetic oligonucleotides were obtained from GENSET. Dephosphorylated primers were 5′-phosphorylated with T4 polynucleotide kinase (New England Biolabs) as described (19). Unreacted [γ-^{32}P]ATP was separated by passing the mixture over a Nensorb-20 column (Du Pont) using the manufacturer's suggested protocol. The photoreactive nucleotide analogues 5-[*N*-(2-nitro-5-azidobenzoyl)-*trans*-3-aminopropenyl-1]-2′-deoxyuridine-5′-triphosphate (NAB-4-dUTP) and 5-[*N*-[*N*-(2-nitro-5-azidobenzoyl)glycyl]-*trans*-3-aminopropenyl-1]-2′-deoxyuridine-5′-triphosphate (NAB-7-dUTP) (see Fig. 1) were synthesized and characterized essentially as described (20).

Primer–template annealing

Primers were annealed to templates at a molar ratio of 1:1 in 10 mM Tris–HCl, pH 7.5, 5 mM EDTA by heating the mixture at 90°C for 3 min and then the mixtures were allowed to cool slowly to room temperature. The sequences of the primers and templates used were as follows (note that the length of the ssDNA extension of the primer–templates depicted below is reduced by 1 nt after incorporation of the photoreactive nucleotide at the 3′-end):

System 1 (31 nt ssDNA extension)
```
5′-TTTTTTTTTTTTGGTTCGATATCGTAGTTCTAGTGTATAGCCCCTACC-3′
                                3′-CACATATCGGGGATGG-5′
```
System 2 (19 nt ssDNA extension)
```
5′-GGTTCGATATCGTAGTTCTAGTGTATAGCCCCTACC-3′
                    3′-CACATATCGGGGATGG-5′
```
System 3 (14 nt ssDNA extension)
```
5′-GATATCGTAGTTCTAGTGTATAGCCCCTACC-3′
                  3′-CACATATCGGGGATGG-5′
```
System 4 (13 nt ssDNA extension)
```
5′-ATATCGTAGTTCTAGTGTATAGCCCCTACC-3′
                3′-CACATATCGGGGATGG-5′
```
System 5 (9 nt ssDNA extension)
```
5′-CGTAGTTCTAGTGTATAGCCCCTACC-3′
          3′-CACATATCGGGGATGG-5′
```
System 6 (4 nt ssDNA extension)
```
5′-TTCTAGTGTATAGCCCCTACC-3′
     3′-CACATATCGGGGATGG-5′
```

Primer elongation in the presence of photoreactive dNTP analogs

Conditions for elongation of oligonucleotides by photoreactive analogs of dNTPs were identical to those used for photocrosslinking. DNA synthesis was initiated by adding polymerase and carried out for 30 min at 25°C. The reaction was terminated by adding 10 µl of 90% formamide, 50 mM EDTA and 0.1% bromophenol blue. The mixture was heated for 3 min at 80°C and products were analyzed by electrophoresis followed by autoradiography (19).

Photochemical crosslinking

RPA was photoaffinity labeled with photoreactive primers synthesized *in situ* using NAB-7-dUTP or NAB-4-dUTP and pol β or KF. Reaction mixtures (10 or 20 µl) contained 50 mM Tris–HCl pH 7.8, 10 mM $MgCl_2$, 50 mM KCl, 1.4 or 2.7 µM pol β or 1 µM KF, 0.2 or 0.8 µM template–5′-^{32}P-primer, 10 µM photoreactive analogs and 0.4–2.4 µM RPA as indicated. The reaction mixtures were incubated at 25°C for 30 min to allow elongation of the primers. Then the mixtures were spotted onto parafilm placed on ice. The samples were then UV irradiated for 20 min with a Bausch and Lomb monochromator equipped with an HBO W super-pressure mercury lamp. UV light of 320 nm was used for crosslinking. Reactions were stopped by adding Laemmli buffer and heating. The photochemically crosslinked protein–DNA samples were separated by SDS–PAGE (21). Dried gels were subjected to autoradiography or quantitated using a PhosphorImager (Molecular Dynamics).

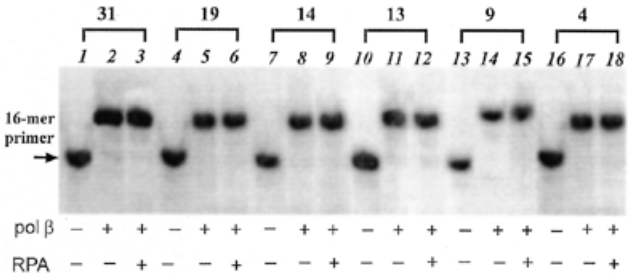

Figure 2. Substrate properties of NAB-7-dUTP. Primer elongation reactions were catalyzed by pol β in the absence or presence of RPA as indicated. The single-stranded extension in numbers of nucleotides after incorporation of the photoreactive nucleotide analog into the template–primer systems is given at the top of the figure. The position of the 16mer primer strand is marked by an arrow in the left margin.

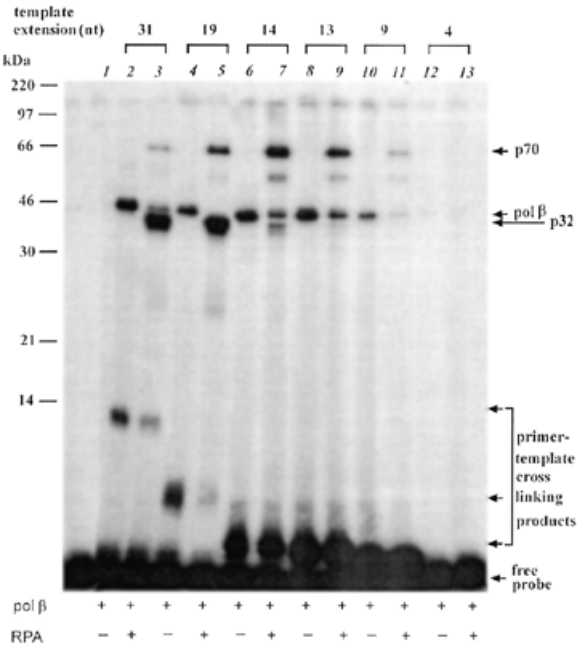

Figure 3. Photoaffinity labeling of RPA by photoreactive primers. Primer elongation reactions using different template–primer structures (0.8 μM each) were carried out by pol β (2.7 μM) in the absence or presence of RPA (0.86 μM). The ssDNA extension in numbers of nucleotides after incorporation of the photoreactive dUTP analog is indicated at the top of the figure for each primer–template system. A control reaction (lane 1) contained pol β, template–primer and RPA without photoreactive nucleotide. After incubation reaction mixtures were UV-irradiated. The crosslinked protein–DNA complexes were separated by SDS–PAGE and visualized by autoradiography. The positions of the free probe as well as crosslinked products and of protein markers are indicated in the right and left margins, respectively.

RESULTS

The structures of base substituted arylazido derivatives of dUTP used in this study are shown in Figure 1. The photoreactive properties of dUTP analogs allow UV irradiation with light at wavelengths >300 nm, which is far beyond the absorbency maxima of nucleic acids and proteins. Indeed, we did not observe enzyme inactivation under these conditions (data not shown). The analogs were shown to be effective substrates of pol β (13,14). We have worked out conditions that allowed us to introduce a single photoreactive moiety into the 3′-end of ^{32}P-labeled photoreactive primers using a primer elongation reaction catalyzed by pol β (Fig. 2). Each of our template–primer systems was equally well elongated with the nucleotide analog (compare lanes 1–3, system 1; lanes 4–6, system 2; lanes 7–9, system 3; lanes 10–12, system 4; lanes 13–15, system 5; lanes 16–18, system 6). We did not detect any influence of RPA on the primer elongation reaction (compare lanes 2 and 3, 5 and 6, 8 and 9, 11 and 12, 14 and 15, and 17 and 18). We, therefore, used these conditions for the synthesis of a photoreactive primer before UV crosslinking in the presence or absence of RPA. One of the most interesting aspects is to identify different RPA conformations depending on the length of ssDNA interacting with RPA.

To determine the single-stranded template extension length that is needed to induce subunit rearrangement around the 3′-end of the primer, we used template–primer systems in which the protruding template tail varied from 4 to 31 nt. Photoreactive dUTP analogs (NAB-4-dUTP and NAB-7-dUTP) were used for primer elongation by pol β. After completing primer elongation in the presence or absence of RPA, reaction mixtures were irradiated with UV light (320 nm). Figure 3 shows a representative experiment of crosslinking efficiencies of RPA subunits to the different template–primer systems when NAB-7-dUTP was used as substrate. In the case of the template extension equal to 31 nt, preferential labeling of p32 with only slight labeling of p70 was seen (lane 3). The natures of crosslinking products were proved by immunoprecipitation assay with specific antibodies against RPA subunits as described (14). The intensity of p70 labeling increased for the 19 nt template extension substrate without a strong decrease in p32 labeling (lane 5). A remarkable increase in p70 labeling was observed with the 14 nt extension, accompanied by a strong decrease in p32 labeling (lane 7). The former effect increased with the 13 nt template extension (lane 9). The labeling of p32 became negligible starting from the template extension equal to 9 nt, whereas slight labeling of the p70 subunit was still detected (lane 11). The DNA duplex with a 4 nt template extension did not reveal any labeling of RPA subunits, arguing for a lack of access to RPA crosslinking under these conditions. A PhosphorImager quantification has confirmed the regularity of the change in subunit crosslinking intensities. We have shown earlier that a DNA duplex with a template extension of one base after elongation with a photoreactive group creating a blunt-ended DNA duplex is unable to label RPA (14). Similar data have been obtained when another photoreactive analog, NAB-4-dUTP, was used for the introduction of a photoreactive group into the 3′-end of the primer (data not shown). The Klenow fragment of DNA polymerase I could replace pol β efficiently in the assays without changing the outcome. However, in that case we were unable to follow p70 subunit labeling because of the overlapping molecular masses of p70 crosslinked to photoreactive primer and the Klenow fragment itself (data not shown).

With each of the template systems used, a decrease in pol β labeling in the presence of RPA compared to its absence is observed (Fig. 3, compare lanes 2 and 3, 4 and 5, 6 and 7, 8 and 9 and 10 and 11). This is in line with previous reports that RPA

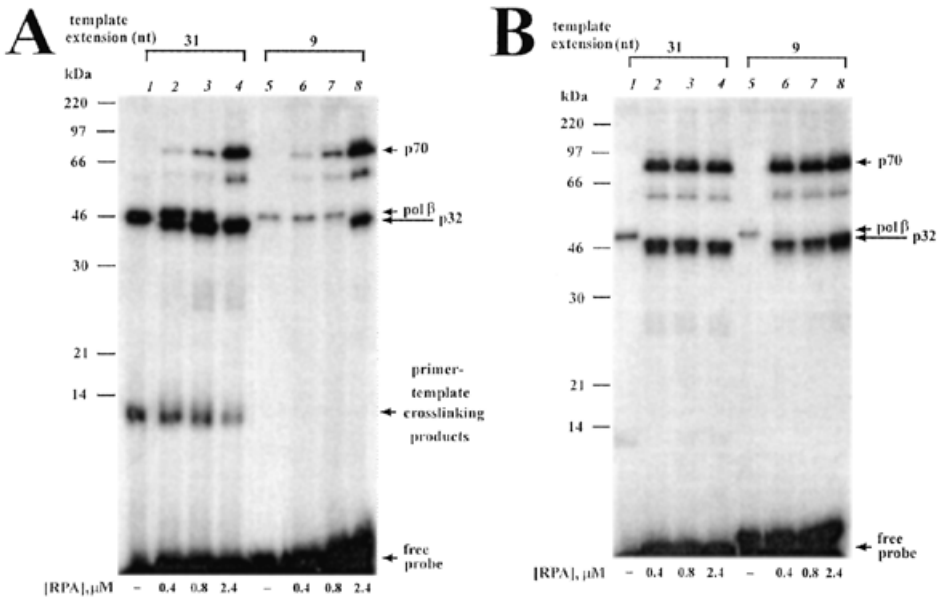

Figure 4. Influence of RPA concentration on photocrosslinking. (**A** and **B**) Photoaffinity labeling of RPA by photoreactive primers was done at different RPA concentrations using template–primer systems that have a template extension of 31 (system 1, lanes 1–4) and 9 nt (system 5, lanes 5–8), respectively, as indicated at the top of the figure. Reaction mixtures were composed of 2.7 μM pol β, 0.8 (A) or 0.2 μM (B) template–primer, 10 μM NAB-7-dUTP and various RPA concentrations ranging from 0.4 up to 2.4 μM as indicated. After incubation reaction mixtures were UV-irradiated. The UV-crosslinked products were separated by SDS–PAGE and visualized by autoradiography. The positions of the free probe as well as crosslinked products and of protein markers are indicated in the left and right margins, respectively.

competes with pol β for binding with the template–primer junction (13,14).

The data presented in Figure 3 demonstrate modification not only of the RPA subunits but also of the template by the photoreactive primer with a photoreactive group at its 3′-end. This should happen when photoreactive DNA duplex is not complexed with pol β or RPA. When RPA was added to the reaction mixtures, the intensity of DNA template modification was lower than in the experiments when pol β was present in the reaction mixtures alone (Fig. 3, compare lanes 2 and 3 and 4 and 5). This is presumably the consequence of RPA binding to the template–primer DNA duplexes. The effect was stronger, however, for DNA duplexes with a long template extension than for those with a short extension of the template strand (Fig. 3, lanes 6–11).

For the experiments shown in Figure 3 we used RPA and DNA at concentrations of 0.84 and 0.8 μM, respectively, which yielded an ~1:1 molar ratio of RPA to DNA duplex. To analyze the RPA arrangement on the DNA we varied the RPA concentration to increase this ratio (Fig. 4). The main idea of these experiments was to increase the stoichiometry of RPA binding to the DNA template, i.e. to bind several RPA molecules to the partial DNA duplex and thus to analyze the effect of cooperative binding on the pattern of RPA subunit labeling.

For the experiments we have varied the RPA concentration between 0.4 and 2.4 μM in the presence of 0.8 (Fig. 4A) or 0.2 μM (Fig. 4B) partial DNA duplexes with extensions of 31 and 9 nt, respectively. The molar RPA to DNA ratios were, accordingly, for Figure 4A: 0.5 (lanes 2 and 6), 1.0 (lane 3 and 7) and 3.0 (lane 4 and 8), and for Figure 4B: 2 (lanes 2 and 6), 4 (lane 3 and 7) and 12 (lanes 4 and 8). Elongation of the primers with NAB-7-dUTP was analyzed separately under conditions used in the crosslinking experiments (see Fig. 2).

Using the 31 nt extended DNA duplex at molar RPA:DNA ratios of 0.5 and 1.0 we observed strong p32 and weak p70 labeling, respectively (Fig. 4A, lanes 2 and 3), with both p32 and p70 labeling slightly increased at the higher RPA concentration. In contrast, with the 9 nt extended template only weak labeling of p70 was detected, which again was slightly stronger in the presence of elevated RPA concentrations (Fig. 4, lanes 6 and 7). With this template, no labeling of the p32 subunit took place. The crosslinking pattern differed substantially when the molar ratio of RPA to partial DNA duplex was 2:1 and higher (Fig. 4A, lanes 4 and 8 and B, lanes 2, 4 and 6–8). In this case, intensive labeling of both subunits (p70 and p32) was observed independent of the length of the DNA template used. Similar data were obtained with the 13 nt extended template (data not shown).

DISCUSSION

To unravel the role of RPA in the various processes of DNA metabolism it might be useful to investigate the binding of RPA to DNA structures other than ssDNA, which mimic more closely the *in vivo* situation. A step forward in this direction was undertaken for the involvement of RPA during nucleotide excision repair (22). Using hairpin structures mimicking damaged DNA, RPA was found to bind ssDNA in a defined polarity. The binding was strong for substrates with a 3′-protrusion and weak for those with a 5′-protrusion. More intriguingly, the polarity of RPA binding determined the ability of RPA to interact with different repair enzymes.

During SV40 DNA replication, the viral large T antigen initiator protein melts 8 bp within the SV40 origin of replication that represents an entry site for RPA (23,24). After more extensive unwinding through the helicase activity of T antigen, creating longer stretches of ssDNA, the cellular DNA polymerase α–primase complex is able to synthesize the first RNA primer, which is then elongated by DNA synthesis (25).

To analyze in detail how the RPA subunit arrangement at the template–primer junction is influenced by the length of the template protrusion, in the present work we used template–primer duplexes with template protrusions ranging in size from 31 to 4 nt. This system could represent a model of the change in RPA conformation that occurs during the course of nascent lagging strand DNA synthesis (8). We will present a model of RPA conformations that act in the replication fork.

The length of the template ssDNA strand determines the orientation of the RPA subunits within the DNA-bound complex

We suppose that the different pattern of subunit labeling observed with varying template tail lengths directly reflects the arrangement of RPA subunits relative to the 3′-end of the primer. When RPA binds to an extended template tail (31 or 19 nt) the p32 subunit is positioned in close proximity to the 3′-end of the primer and restricts p70 subunit contact to solely with the ssDNA part. In contrast, with shorter extensions (14, 13 or 9 nt) the accessibility of p32 to the 3′-end is significantly decreased, allowing the p70 subunit to approach the primer end more closely. It is likely that the orientation of the p32 subunit in relation to the 3′-end of the primer is determined by the interaction of p70 with the single-stranded template strand. This is supported by the experiments in which individual subunits of RPA were used in similar crosslinking experiments. Only in the case of p70 was DNA binding found (26).

In accordance with the different RPA–ssDNA complexes visualized by scanning electron microscopy (11), we suggest that RPA complexes formed with DNA templates having long (31 or 19 nt), medium (14 or 13 nt) and short (9 nt) template tail lengths adopt elongated extended, elongated contracted and globular shapes, respectively. Globular complexes replace elongated ones as the DNA contact size decreases from 31 to 8 nt, resulting in a functional transition to unstable DNA binding. As depicted in the model (Fig. 5), p32 would accordingly contact (Fig. 5A), be close to (Fig. 5B) or far from (Fig. 5C) the primer end. It is worth mentioning that p32 becomes accessible for phosphorylation by DNA-PK only in the elongated extended conformation (Fig. 5A; 4). Positioning of the p32 subunit depends on how extensive the p70 contacts with DNA are. p70 possesses three independent binding sites (2), of which domain A is stable enough for band shift experiments, while domains B and C need crosslinking to be revealed in this assay (2; K.Weisshart, unpublished results). In addition, crystallographic analysis using an 8 nt ssDNA template revealed major contacts made by domain A, whereas domain B contributed fewer sites for DNA binding (3). Hence, we favor a model in which the first contacts of RPA with DNA are made by domain A. Then, dependent on the template configuration, the other two domains can also make contacts. Through this engagement of different DNA binding domains of RPA, the complex adopts its special conformation, which serves special functions during the replication process. It is intriguing that p32 also harbors a DNA binding domain, domain D, but that this binding domain can access DNA only in the context of the heterotrimer or if the subunit is truncated (3,6,7,14).

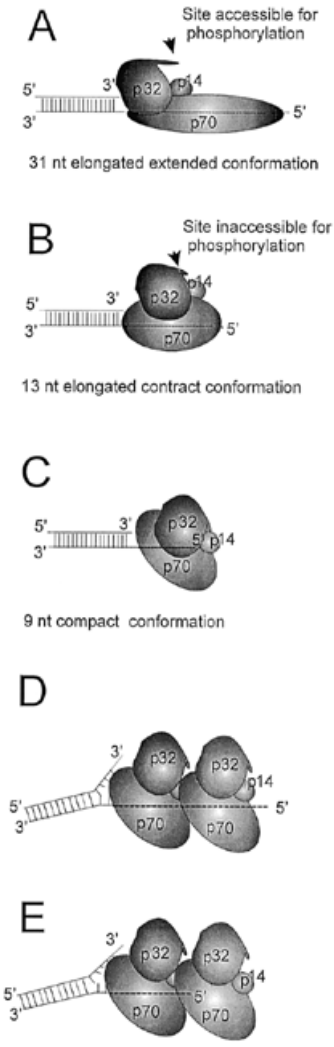

Figure 5. Model of RPA–DNA interactions. (**A**, **B** and **C**) The RPA structures adopted in the elongated extended, elongated compact, and globular compact form according to the size of the ssDNA template tail. Note that only in the extended form can the N-terminus of the p70 subunit become available and p32 make close contacts with the primer terminus. (**D** and **E**) Cooperative binding induces RPA oligomers to partially unwind the duplex region, allowing more RPA molecules to bind per ssDNA length.

Cooperative interactions determine the binding mode of RPA to DNA

Human RPA binds DNA with low cooperativity (27,28). We have used excess RPA to DNA to analyze the influence of cooperativity of RPA binding on its subunit arrangement near the 3′-end of the primer. Intriguingly, when RPA was in excess over DNA we detected a different pattern of RPA subunit labeling than is the case when working under stoichiometric conditions. We found similar intensities of labeling of both the p70 and the p32 subunits (Fig. 4) even with the templates harboring a short

tail, which otherwise show hardly any p32 labeling. The pattern of RPA subunit labeling observed under excess RPA over DNA could be a consequence of cooperative interaction of RPA molecules that brings about a change in RPA conformation. We suppose that a cooperativity-dependent transition in conformation may take place independently of one or more partners bound to DNA. Another, and even more reasonable, explanation is the assumption of a DNA unwinding action of RPA. A DNA destabilizing activity, which is able to unwind long stretches of DNA duplex, has been shown earlier (5,26,29,30). A practically identical pattern of subunit labeling observed with short (9 nt) and long (31 nt) template tails in the case of RPA excess suggests DNA unwinding rather than merely a conformation transition. We suppose that the RPA molecule nearest to the 3′-end can destabilize the double strand, allowing further invasion of a region of former duplex and providing additional room for the second RPA molecule, which in addition stabilizes the RPA–DNA complex. RPA-stimulated fraying of the 3′-end of a DNA duplex was demonstrated by experiments with replicating SV40 chromatin (8). Our data give significance to the finding that the size of the melted bubble within the T antigen–ori complex is ~8 nt. Relatively stable RPA binding to ssDNA of such a size probably demands cooperative interactions with another RPA molecule (10). Therefore, when one RPA molecule binds to ssDNA with weak affinity, cooperative binding of an additional RPA molecule would significantly strengthen the 8–10 nt RPA interaction.

Interaction of RPA with DNA during the process of DNA replication

The different conformations adopted by RPA during DNA binding as described above may be significant for the replication process. After initial opening of the replication origin by 8 bp by an initiation protein, RPA will engage with the bubble structure created in the globular form and assist further unwinding (26). After more extensive unwinding by a helicase, RPA will adopt a more elongated configuration, allowing the p32 subunit to contact the primer end synthesized by the DNA polymerase α–DNA primase complex. In this state, the function of p32 can be regulated by phosphorylation. As the template ssDNA region becomes very small in the course of nascent DNA synthesis at the lagging strand, RPA would transit to the globular state and p32 would as a consequence disengage from the primer. As a consequence, the RNA–DNA primers face small gaps at their 3′-ends as suggested by the Nested Discontinuity Model (8,31,32). Since the globular state binds DNA with low affinity, it gives RPA the opportunity to leave the DNA, enabling the gap to be filled. This model is in agreement with results obtained for SV40 replicating chromosomes, where p32 was shown to disengage from the primer end when the RNA–DNA primers reach their mature length (8).

The different modes of RPA binding speak in favor of a very dynamic role for RPA in DNA metabolism rather than only being required to stabilize ssDNA structures in the course of DNA synthesis. It is very likely that RPA modulates specific DNA structures at various stages of DNA metabolism and regulates loading of enzymes and factors involved in DNA replication, repair and recombination.

ACKNOWLEDGEMENTS

The authors are grateful to Gabriel Kaufmann for contributing fruitful discussions of our results and to Richard d'Ari for careful reading of the manuscript. This work was supported in part by an INTAS grant (96-1778) and by a grant from the Russian Foundation for Basic Research (98-04-49718).

REFERENCES

1. Wold,M.S. (1997) *Annu. Rev. Biochem.*, **66**, 61–62.
2. Brill,S.J. and Bastin-Shanower,S. (1998) *Mol. Cell. Biol.*, **18**, 7225–7234.
3. Bochkarev,A., Pfuetzner,R.A., Edwards,A.M. and Frappier,L. (1997) *Nature*, **385**, 176–181.
4. Walther,A.P., Gomes,X.V., Lao,Y., Lee,C.G. and Wold,M.S. (1999) *Biochemistry*, **38**, 3963–3973.
5. Lao,Y., Lee,C.G. and Wold,M.S. (1999) *Biochemistry*, **38**, 3974–3984.
6. Bochkareva,E., Frappier,L., Edwards,A.M. and Bochkarev,A. (1998) *J. Biol. Chem.* **273**, 3932–3936.
7. Philipova,D., Mullen,J.R., Maniar,H.S., Lu,J., Gu,C. and Brill,S.J. (1996) *Genes Dev.*, **10**, 2222–2233.
8. Mass,G., Nethanel,T. and Kaufmann,G. (1998) *Mol. Cell. Biol.*, **18**, 6399–6407.
9. Alani,E., Thresher,R., Griffithand,J.D. and Kolodner,R.D. (1992) *J. Mol. Biol.*, **227**, 54–71.
10. Blackwell,L.J. and Borowiec,J.A. (1994) *Mol. Cell. Biol.*, **14**, 3993–4001.
11. Blackwell,L.J., Borowiec,J.A. and Mastrangelo,I.A. (1996) *Mol. Cell. Biol.*, **16**, 4798–4807.
12. Sibenaller,Z.A., Sorenson,B.R. and Wold,M.S. (1998) *Biochemistry* **37**, 12496–12506.
13. Lavrik,O.I., Kolpashchikov,D.M., Nasheuer,H.-P., Weisshart,K. and Favre,A. (1998) *FEBS Lett.*, **441**, 186–190.
14. Lavrik,O.I., Nasheuer,H.-P., Weisshart,K., Wold,M.S., Prasad,R., Beard,W., Wilson,S.H. and Favre,A. (1998) *Nucleic Acids Res.*, **26**, 602–607.
15. Beard,W.A. and Wilson,S.H. (1995) *Methods Enzymol.*, **262**, 98–107.
16. Joyce,C.M. and Grindley,N.D. (1983) *Proc. Natl Acad. Sci. USA*, **80**, 1830–1834.
17. Henricksen,L.A. and Wold,M.S. (1994) *J. Biol. Chem.*, **269**, 24203–24208.
18. Nasheuer,H.-P., von Winkler,D., Schneider,C., Dornreiter,I., Gilbert,I. and Fanning,E. (1992) *Chromosoma*, **102**, 52–59.
19. Sambrook,J., Fritsch,E.F. and Maniatis,T. (1989) *Molecular Cloning: A Laboratory Manual*, 2nd Edn. Cold Spring Harbor Laboratory Press, Cold Spring Harbor, NY.
20. Wlassoff,W.A., Dobrikov,M.I., Safronov,I.V., Dudko,R.Y, Bogachev,V.S., Kandaurova,V.V., Shishkin,G.V., Dymshits,G.M. and Lavrik,O.I. (1995) *Bioconjugate Chem.*, **6**, 352–360.
21. Laemmli,U.K. (1970) *Nature*, **277**, 680–685.
22. De Laat,W.L., Appeldorn,E., Sugasawa,K., Weterings,E., Jaspers,N.G.J. and Hoeijmakers,J.H.J. (1998) *Genes Dev.*, **12**, 2598–2609.
23. Iftode,C. and Borowiec,J.A. (1997) *Mol. Cell. Biol.*, **17**, 3876–3883.
24. Iftode,C. and Borowiec,J.A. (1998) *Nucleic Acids Res.*, **26**, 5636–5643.
25. Tsurimoto,T., Fairman,M.P. and Stillman,B. (1989) *Mol. Cell. Biol.*, **9**, 3839–3849.
26. Kolpashchikov,D.M., Weisshart,K., Nasheuer,H.-P., Khodyreva,S.N., Fanning,E., Favre,A., Lavrik,O.I. (1999) *FEBS Lett.*, **450**, 131–134.
27. Kim,Ch., Paulus,B.F. and Wold,M.S. (1994) *Biochemistry*, **33**, 14197–14206.
28. Kim,Ch. and Wold,M.S. (1995) *Biochemistry*, **34**, 2058–2064.
29. Georgaki,A., Strack,B., Podust,V. and Hubscher,U. (1992) *FEBS Lett.*, **308**, 240–244.
30. Treuner,K., Rampsberger,U. and Knippers,R. (1996) *J. Mol. Biol.*, **259**, 104–112.
31. Nethanel,T., Zlotkin,T. and Kaufmann,G. (1992) *J. Virol.*, **62**, 6634–6640.
32. Salas,M., Miller,T.J., Leis,J. and DePamphilis,M.L. (1996) In DePamphilis,M.L. (ed.), *DNA Replication in Eukaryotic Cells*. Cold Spring Harbor Laboratory Press, Plainview, NY, pp. 131–176.